Classification for Avian Malaria Parasite Plasmodium Gallinaceum Blood Stages by Using Deep Convolutional Neural Networks

Veerayuth Kittichai
King Mongkut's Institute of Technology Ladkrabang
Morakot Kaewthamasorn
Chulalongkorn University
Suchansa Thanee
Chulalongkorn University
Rangsan Jomtarak
Suan Dusit University
Kamonpob Klanboot
King Mongkut's Institute of Technology Ladkrabang
Kaung Naing
King Mongkut's Institute of Technology Ladkrabang
Teerawat Tongloy
King Mongkut's Institute of Technology Ladkrabang
Santhad Chuwongin
King Mongkut's Institute of Technology Ladkrabang
Siridech Boonsang (siridech.bo@kmitl.ac.th)
King Mongkut's Institute of Technology Ladkrabang

Research Article

Keywords: Plasmodium gallinaceum, blood stages, egg production, Computer-aided diagnosis

Posted Date: May 10th, 2021

DOI: https://doi.org/10.21203/rs.3.rs-282527/v2

Version of Record: A version of this preprint was published at Scientific Reports on August 19th, 2021.
See the published version at https://doi.org/10.1038/s41598-021-96475-5.

Abstract

The infection of an avian malaria parasite (*Plasmodium gallinaceum*) in domestic chickens presents a major threat to the poultry industry because it causes economic loss in both the quality and quantity of meat and egg production. Computer-aided diagnosis has been developed to automatically identify avian malaria infections and classify the blood infection stage development. In this study, four types of deep convolutional neural networks, namely Darknet, Darknet19, Darknet19-448 and Densenet201 are used to classify *P. gallinaceum* blood stages. We randomly collected a dataset of 12,761 single-cell images consisting of four parasite stages from ten-infected blood films stained by Giemsa. All images were confirmed by three well-trained examiners. The study mainly compared several image classification models and used both qualitative and quantitative data for the evaluation of the proposed models. In the model-wise comparison, the four neural network models gave us high values with the mean average accuracy of at least 97%. The Darknet can reproduce a superior performance in the classification of the *P. gallinaceum* development stages across any other model architectures. Furthermore, the Darknet has the best performance in multiple class-wise classification, with average values of greater than 99% in accuracy, specificity, and sensitivity. It also has a low misclassification rate (< 1%) than the other three models. Therefore, the model is more suitable in the classification of *P. gallinaceum* blood stages. The findings could help us create a fast screening method to help non-experts in field studies where there is a lack of specialized instruments for avian malaria diagnostics.

Introduction

Avian malaria, a mosquito-borne disease, is one of the most common veterinary threats in tropical regions, including South East Asia and South Asia [1]. *Plasmodium gallinaceum* is an important causative agent of avian malaria, which causes more than 80% mortality if left untreated [2]. The disease entails an economic and agricultural loss in poultry processes systems such as poor quality and quantity of meat and egg production[1]. Early and rapid routine screening for a safe and low-cost parasite infection may help prevent transmissions of the disease. Microscopic inspection is a gold standard approach and is widely used to examine and identify avian malaria-infected blood stages under thin-blood film examinations, the outcome of which is validated by highly trained and qualified technicians[3]. Nevertheless, the precise outcome of the above-mentioned procedure depends on the consistency of blood smearing and staining process. In addition, asymptomatic with low parasite infection can be time-consuming and may be undetectable or questionable as a result of inter/intra examiner variability [3]. In addition, unspecific clinical symptoms of avian malaria, such as anorexia, anemia, and green stools, are often seen [1,4]. While most of the nucleic acid-based amplification process, such as the polymerase chain reaction (PCR) assay, is an efficient method with a high sensitivity and malaria detection specificity, it requires an optimal consistency of genomic DNA and expensive tools such as thermocycler and electrophoresis apparatus [5–7]. A professional molecular biologist is also required for further verification of the analysis. Consistently, the molecular biology approach could not always be affordable in low-income and resource-limited nations. As a result, an automated identification tool is desired

Artificial intelligence (AI) technology is currently a positive integration success in a diverse area of interest, including agriculture, medicine and veterinary medicine [8–15]. Computer-aided diagnosis, AI subdivision, have been developed to identify human malaria infections and to classify their blood stage of the parasite growth. These can be used to assist clinical decision-making. Machine learning applications have also been studied in the documented veterinary field [16]. Previous research have suggested a diagnostic tool in veterinary medicine focused on image analysis using machine learning techniques [17,18], such as fish disease diagnosis based microscopic method [19]. The analysis referred to above is intended to enhance the inspection of the pathogen region in the image by means of object detection, which includes various image processing techniques, including noise reduction, edge detection, morphological operations and context extraction.

Deep learning is a revolutionary and groundbreaking approach that has been developed to incorporate a microscopic analysis for the veterinary medicine field [20,21]. The methods are combined and tailored for individual datasets that differ in size of the region of interest. In specific, deep learning technology is applied to end-to-end methods of extraction of features and self-discovery. The deep learning algorithm is very popular and useful with the emergence of a high-power computing machine to be used to study the classification of images and the recognition of clinical issues. Several neural network models have been used to contend with the animal sector, Single-Shot MultiBox Detector (SSD) model used to evaluate the percentage of reticulocytes in cat's samples [22], Alexnet for classification of fish dissease such as Epizootic ulcerative syndrome (EUS), Ichthyophthirius (Ich) and Columnaris.[19]. The works described above makes it possible to apply deep learning algorithms in the field of veterinary medicine.

Previously, several techniques for image-based identification and classification of malaria parasite infections have been discussed, such as dark stretching technique [23], modified fuzzy divergence technique, segmentation techniques [24], adaptive color segmentation and tree-based decision classification [25], segmentation, feature extraction, and SVM classifier [26], convolutional neural classification [27,28]. Moreover, deep CNN research have been conducted under the channel color space segmentation method [29], deep belief network technique [30], the Faster Region-based Convolutional Neural Network (Faster R-CNN) [31], and the MATLAB-based Zach Threshold process for segmentation technique [32]. Successfully, several studies have reported that the use of deep learning models to classify malaria parasites as automatic, rapid, and accurate approaches[33–35]. Interestingly, more than 95% of the accuracy is recorded in the detection of malaria-infected cells using three well-known CNNs, including LeNet, AlexNet, and GoogLeNet [36]. The previous work demonstrated micro-platforms to study and identify the infected avian red blood cell by using morphological modifications on the RBC surface to reveal the phases of *P. gallinaceum*. Since malaria has been described as a disease of blood and blood-forming tissues, the blood film sample has been diagnosed to better understand different degrees of disease [37]. Early rapid screening of parasite infection with reliable and also low cost development is required, which could help us deter the spread of the disease. Therefore, timely identification of malaria parasite in a blood smear test is crucial because it needs reliable and early diagnosis for successful containment [24].

A hybrid platform (VGG19 and SVM) recently demonstrated high performance in detecting infected and non-infected malaria parasite images, as observed follows: 93.44 per cent sensitivity; 92.92 per cent specificity; 89.95 per cent precision, 91.66 per cent F-score and 93.13 per cent accuracy [38]. The outstanding performance of the hybrid algorithms mentioned previously motivates us to develop a hybrid object detection and classification method for further classifying avian malaria in Thailand.

In this work, we employ two-state learning techniques, which combine an object detection model based on YOLOv3 with one of four classification models, namely Darknet, Darknet19, Darknet19-448, and Densenet201, to characterize the avian malaria blood stages of *P. gallinaceum*. This contributes to the study's key contribution, which is to compare various image classification models using blood protozoa photographs, as qualitative and quantitative evidence for evaluating the proposed models. We compare the proposed model's performance to assist in the prediction of parasitized and healthy chicken RBCs in thin blood film photos. The stage of malaria progression would then be estimated, which determines the degree of infection as well as the probability of malaria transmission. In addition to author's knowledge, this research work is the first time that the CNNs deep learning model has been incorporated into the classification of clinical datasets relevant to clinical problems in *P. gallenaceum*-infected chicken. The study result would be useful for the disease diagnosis method in the poultry industry.

Methods

Ethics statement

Archived Giemsa-stained thin-blood films have been collected from previous studies [1,39]. This study was reviewed and approved by the Chulalongkorn University Faculty of Veterinary Science Biosafety Committee (Approval No. 1931011) and was approved by the Institutional Animal Care and Use Committee in accordance with university regulations and policies governing the care and use of laboratory animals (Approval No.1931091). In this study, we strictly adhered to the university's relevant guidelines and regulations.

Data collections

The parasite infection was confirmed by three well-trained investigators using a microscopic diagnosis. Ten *P. gallinaceum*-infected chicken blood films were randomly chosen. A total of 432 images of chicken blood cells at various stages of malarial growth were taken at 1000x using an oil immersion magnification mounted to a light microscope (Olympus CX31, Tokyo, Japan).The digitized chicken blood cells were captured using an Olympus DP21-SAL digital camera (Tokyo, Japan). An individual RBC image from each blood film was selected to be used in an image with a region of interest to the so-called monolayer area.

A hybrid two-stage model: RBC detection and classification models

The proposed methodology for classifying the blood stages of avian malaria, *P. gallenaceum*, using a hybrid two-stage model (object identification YOLOv3 and Darknet/ Densenet201 classification algorithms). Previously, the combination of two CNN models was reported to have increased prediction accuracy[40,41]. In this work, the first stage of the proposed model is the YOLOv3-based object detection, which aims to distinguish a single RBC image from those inside a microscopic image. Among other object detection models, the YOLOv3 model outperformed the others, in terms of localization and classification accuracy[14]. Model inference, in particular, can be accomplished in real-time by processing 45–155 frames per second. It can also recognize up to 9000 object classes. After encoding the circumstantial information of the relative classes, the model can detect the entire area of an input image set with only a few false positives [42] and shows a balance of the accuracy and speed in a practical applications that time is not restrictive [43].

Cropped images (single RBC) from its first stage model inference were used as inputs for the second stage model. The classification model was used in the second stage to categorize the single RBC detected. CNN model candidates were widely used for studying the image classification, from a top-5 pre-trained model which was measured as single-crop validation accuracy at 94.7% [44]. The models employed in this study are the top ranking of the ILSVRC2016 ImageNet competition to identify pathological tasks. These versions are in the following sizes; Densenet201, Darknet, Darknet19, and Darknet19-448 [44]. The model prediction was automatically masked and colored with a JET color map generated by the Class Activation Map (CAM) algorithm [45].

Dataset preparation

Two dataset were developed by a team of experts who labeled all 432 microscopic examination images for RBCs [1,39]. The first dataset is obtained from microscopic images of chicken RBCs scattered around the whole image. A rectangular bounding box closely fitting to the RBC image region was manually designated to each individual RBC. The ground truth data file was saved as a collection of RBCs with designated bounding boxes. The first dataset was then set as the ground truth file for object detection model (YOLOv3). The ground truth was deposited as shown in this link as followed; https://git.cira-lab.com/cira-medical/classification-of-avian-malaria-parasite. Using the first dataset, the YOLOv3 model was subsequently employed to learn and detect individual RBC. By feeding all microscopic images to the trained YOLOv3, the model output reported all of the image region that contained any chicken's RBC. Where an RBC was detected, the image region of a single RBC (both normal and parasitized-RBCs) was cropped using the standard image crop technique. Each single RBC image was then used for the preparation of the second dataset (Fig. 1).

The deep learning classification model was used in the second stage to identify a specific relative class within the cropped image extracted from the captured image containing single chicken's RBC. The second dataset consists of 12,761 cropped images contained a significant proportion of regions of interest (ROI). Pooled single cropped-cell images were grouped and assigned label according to four classes based on their physiological and morphological stages including of: (i) normal RBC for 6,724, (ii) trophozoite for

5,343, (iii) schizont for 657, and (iv) gametocyte for 37, respectively. Each class above was randomly divided for training (90 per cent) and testing (10 per cent) sets, minimizing potential similarities between these two sets. This protocol can be trustable for preventing the sample selection bias from the same patient's slides. While disproportionate sample size between classes has been identified and can trigger biased-prognosis against a class with a large number of image sets, deep learning approach with multi-layered layers and data annotation can be explored prior to model training. To speed up model convergence, rescale the image from raw pixels to 448 x 448 pixels before training with a chosen neural network model.

Data augmentation and model training

Data augmentation techniques were introduced to the dataset prior to training to avoid over-fitting of the training image collection, and it was also used in the case of an unbalanced class. The technique involves rotations, brightness/ contrast, blueness and Gaussian noise as following conditions:

1. The rotational angle was performed with the degree value specified from − 180º to 180º, varied at every 45°.
2. The brightness and contrast were adjusted by multiplying all pixel values for seven steps, ranging 0.4 to 1.6.
3. The Gaussian noise distribution was applied for helping the model to distinguish an original image from the annotated image with We used 5 steps accompanying to 5-standard deviation (σ = 0, 4, 8, 12 16 and 20).

And (iv) Gaussian blur was used to vary the image's sharpening to blurring with 5 steps (Gaussian filter) with a standard deviation of 5, ranging of 1–10.

These models mentioned above were trained on the in-house deep learning platform CiRA CORE (https://git.cira-lab.com/cira/cira-core), under Ubuntu version 16.04, 16 GB RAM, and NVIDIA GeForce GTX1070Ti graphic processor unit. Furthermore, the qualified models were trained for at least 100,000 epochs in order to record the learned parameters. The likelihood of a threshold greater than and equal to 50% is considered to be a true positive value, which incur no cost [41,43]. Otherwise, result of image classification would produce false positive values that is unexpected in medical diagnosis.

Model evaluations

The performance quality of the model- and class-wise prediction were evaluated in terms of the following statistical metric parameters: accuracy, sensitivity, specificity, and misclassification rate [11,41,46].

$$Sensitivity = \frac{TP}{TP + FN}$$

1

……

$$Specificity = \frac{TN}{TN + FP}$$

2

……..

$$Accuracy = \frac{TP + TN}{TP + TN + FP + FN} \ldots\ldots\ldots\ldots\ldots\ldots\ldots\ldots\ldots\ldots\ldots\ldots (3)$$

$$Missclassificationrate = \frac{FP + FN}{TP + TN + FP + FN} \ldots\ldots\ldots (4)$$

where TP is the number of true positive values, TN is the number of true negative values, FP is the number of false positive values, and FN is the number of false negative values.

Confusion matrix table was created to demonstrate the overall accuracy of both the model capability in the multi-class classification. An area under the Receiver Operating Characteristic (ROC) curve (AUC) at 95% confident of interval (CI) was designed to calculate the average accuracy of the model using python software.

Results

Accompanying those protocol in the method part, we combined YOLOv3 and image classification (Darknet/ Densenet201) models in order to localize, identify and classify a single RBC cells from any microscopic examination image with multiple-RBC cells. Their relative RBC's classes were then classified from both normal and that infection varied based on pathological features (Fig. 2). It was more beneficial when a combination of two deep learning models such as using two-state learning strategies of concatenated YOLO models for identifying genus, species and gender of the mosquito vector [41]. Besides, the hybrid platform of YOLOv2 with ResNet-50 detector which help improve the average precision of the proposed detector up to 81% compared to a previous single model [40].

Performance comparison of classification models

In this analysis, the model-wise performance was assessed as to whether the classification model was the best-selected model based on an attention map and used to estimate *P. gallinaceum*-infected blood phases (Fig. 2). These models included Darknet, Darknet19, Darknet19-448 and Densenet201 as described above. For classification models for avian malaria parasite phases, performance metrics such as average precision, uncertainty confusion matrix table, and ROC curve were estimated and compared. In addition, we randomly split the single-cell images for training and comparing the image sets to determine if the different models generated the same classifier performance. All well-trained models provided us with high average accuracy values of more than 97 percent, which increased to 99.2 percent for the Darknet algorithm (Table 1). In addition, all other two statistics also support the Darknet network as a superior performance at 99.2 per cent for both sensitivity and specificity, respectively (Table 2 and

Table 3). Interestingly, all models used showed less than 2% error rate, which was particularly impressive considering that the Darknet network gave less than 1% error rate (Table 4).

Table 1
Model-wise comparison and multiclass-wise comparison based on the accuracy from one-class versus total.

DCNNs	Average	Normal	Trophozoite	Schizont	Gametocyte
Darknet	0.992	0.983	0.983	1.000	1.000
Darknet19	0.991	0.981	0.981	1.000	1.000
Darknet19_448	0.984	0.967	0.967	1.000	1.000
Densenet201	0.979	0.963	0.957	0.994	1.000

Table 2
Model-wise comparison and multiclass-wise comparison based on the sensitivity from one-class versus total.

DCNNs	Average	Normal	Trophozoite	Schizont	Gametocyte
Darknet	0.992	0.974	0.992	1.000	1.000
Darknet19	0.991	0.972	0.990	1.000	1.000
Darknet19_448	0.982	0.972	0.957	1.000	1.000
Densenet201	0.977	0.966	0.940	1.000	1.000

Table 3
Model-wise comparison and multiclass-wise comparison based on specificity from one-class versus total.

DCNNs	Average	Normal	Trophozoite	Schizont	Gametocyte
Darknet	0.992	0.993	0.976	1.000	1.000
Darknet19	0.992	0.991	0.975	1.000	1.000
Darknet19_448	0.984	0.962	0.975	1.000	1.000
Densenet201	0.981	0.960	0.969	0.994	1.000

Table 4
Model-wise comparison and multiclass-wise comparison based on misclassification rate from one-class versus total.

DCNNs	Average	Normal	Trophozoite	Schizont	Gametocyte
Darknet	0.009	0.017	0.017	0.000	0.000
Darknet19	0.010	0.019	0. 019	0.000	0.000
Darknet19_448	0.017	0.033	0. 033	0.000	0.000
Densenet201	0.022	0.037	0.043	0.006	0.000

Table 5. Comparison of the studied model performance using the confusion matrix table.

Table 5.1 The confusion matrix table of using Darknet model.

Darknet	Normal	Trophozoite	Schizont	Gametocyte
Normal	594 (97.38%)	4 (0.83%)	0 (0.00%)	0 (0.00%)
Trophozoite	16 (2.62%)	480 (99.17%)	0 (0.00%)	0 (0.00%)
Schizont	0 (0.00%)	0 (0.00%)	60 (100.00%)	0 (0.00%)
Gametocyte	0 (0.00%)	0 (0.00%)	0 (0.00%)	5 (100.00%)

Table 5.2 The confusion matrix table of using Darknet19 model.

Darknet19	Normal	Trophozoite	Schizont	Gametocyte
Normal	593 (97.21%)	5 (1.03%)	0 (0.00%)	0 (0.00%)
Trophozoite	17 (2.79%)	479 (98.97%)	0 (0.00%)	0 (0.00%)
Schizont	0 (0.00%)	0 (0.00%)	60 (100.00%)	0 (0.00%)
Gametocyte	0 (0.00%)	0 (0.00%)	0 (0.00%)	5 (100.00%)

Table 5.3 The confusion matrix table of using Darknet19-448 model.

Darknet19-448	Normal	Trophozoite	Schizont	Gametocyte
Normal	593 (91.21%)	21 (4.34%)	0 (0.00%)	0 (0.00%)
Trophozoite	17 (2.79%)	463 (95.66%)	0 (0.00%)	0 (0.00%)
Schizont	0 (0.00%)	0 (0.00%)	60 (100.00%)	0 (0.00%)
Gametocyte	0 (0.00%)	0 (0.00%)	0 (0.00%)	5 (100.00%)

Table 5.4 The confusion matrix table of using Darknet19-448 model.

Densenet201	Normal	Trophozoite	Schizont	Gametocyte
Normal	589 (96.56%)	22 (4.55%)	0 (0.00%)	0 (0.00%)
Trophozoite	21 (3.44%)	455 (94.01%)	0 (0.00%)	0 (0.00%)
Schizont	0 (0.00%)	7 (1.45%)	60 (100.00%)	0 (0.00%)
Gametocyte	0 (0.00%)	0 (0.00%)	0 (0.00%)	5 (100.00%)

General accuracy, obtained from the confusion matrix table, showed outstanding values all four models (Table 5). In addition, the Darknet model outperformed all other models by more than 97 percent (Table 5.1–5.4). Overall, the general accuracy from the confusion matrix gave greater than 95 per cent, except for the Darknet19-448 for classifying the normal RBC class and followed by the DenseNet201 for classifying the trophozoite class gaves us at 91.21 and 94.01 per cent, respectively (Table 5.3 and Table 5.4). Specifically, this manifested in an overall AUC ranking of 0.986–1.000 (Fig. 3). Hence, the Darknet models can reproduce superior performance in the classification of the development phases of *P. gallinaceum* in every other model architectures.

Multiple class comparison

Based on the best-selected network model, an interpretation of the classification outcome produced an empirical result in distinguishing the malaria parasite stages. Despite training the model with disproportionate sample sizes across classes, the neural network model's multiple class-wise consistency demonstrated great statistical values for all classes, with greater than 99 percent of all output matrices used showing no bias against either class (Table 1–3). This is due to the fact that our best-chosen model can distinguish malaria phases with a low rate of misclassification of less than 1% (Table 4). This may be one of the benefits of applying the class-balancing data augmentation protocol to the prepared dataset. This study's findings indicate that the model could be validated using multiple blood smears derived from real-world contexts.

Discussion

In this study, the robustness of deep neural network models leads to the discovery of a new approach for more rapid screening of avian malaria under a microscope. Asymptomatic diseases, in particular, can lead to disease transmission and even death if not adequately prevented. [47,48]. This study may contribute to main comparison of several image classification models based on images of avian malaria, *P. gallenaceum*. Also, both qualitative and quantitative data were used to evaluate the performance of the proposed models.

Several CNNs has also been developed to provide a number of pre-trained ImageNet classification models, including AlexNet, Darknet, VGG-16, Resnet [49], ResNext, and Densenet201 [50], for use as effective in image classification applications. According to an evaluation of the performance of these pre-trained models, Darknet model has a higher accuracy than Densenet201 model and also provides the fastest processing time in both CPU and GPU [44,51]. Despite the fact that we trained network models with actual patient-level yet unbalanced class sizes, the performance of well-trained proposed models has shown an outstanding outcome based on several statistical parameters, even in a multi-class comparison. Since the project was a significant success this would help to advance the development of innovative technologies in order to implement and validate it in a real-world environment.

We would like to illustrate our approach to developing deep learning models from concatenated neural network architectures to make clinical applications by viewing the video as follow:

https://www.youtube.com/watch?v=xq1ZGdgHrMA. Nonetheless, before the technology is implemented, the inter- and intra-variability examinations should be performed in order to validate the degree of consensus between the predictive model's functional performance metrics and the human expert [52].

Limitation of the study is deeply based on the determination of three key points for the preparation of the dataset [53], including; (i) differences in the parasite-blood stages [54], (ii) infection status that can induce either single or multiple infections, and (iii) co-infections in any single blood cell. The imbalance data is another consequence of dataset preparation, though it is less severe than the others listed above. In the case of differences in the blood stage of each parasite, an increasing number of sample is a potential solution, however the analysis has had an effect on model efficiency under the research design. This may be because the image set is a special attribute between classes that helps to increase class differentiation for the well-trained models. We have different sizes of tested set including 610, 484, 60 and 5 images for normal RBC-, trophozoite-, schizont-, and gametocyte classes, respectively. Although our datasets used are imbalance, in the study, the overall accuracy shows more than 98–100% in classifying between the independently different classes. Since our models were trained utilizing the well-planned dataset preparation described in the method section, the role of data augmentation and data balancing for environment simulation improved the classification efficiency[46]. Furthermore, we appropriately chose an image of almost a single stage of parasite infection to be examined. Since the staining of artefacts/impurities of uninfected blood cells can interfere with the prediction, the expert's simple staining of color under the Giemsa staining process also provides us with the ideal dataset [55]. Nevertheless, the model must be validated in a specific environment of multiple pathogens and co-infections, which could already exist in field samples.

Conclusions

In this study, the application of a deep neural learning network to identify and verify avian malaria and also to assess it by using truly invisible images that have never been published. Based on our results, we demonstrated the superior performance of a novel hybrid two-stage model (object detection YOLOv3 and Darknet/ Densenet201 classification algorithms). Regardless of the fact that we trained network models with real patient-level yet unbalanced class sizes, the performance of well-trained proposed models was exceptional based on many statistical parameters, including in a multi-class comparison. Furthermore, we can deduce that only a model learning methodology and data preparation should be used in the research design. Fortunately, the study showed a high value of the various statistical measurements listed above, which could be useful for cytological technicians in making decisions. It would be useful to diagnosis malaria infections wherever it is due to a shortage of molecular biology and veterinary knowledge.

Declarations

Data availability

The data that support the findings of this study are available from the corresponding author's GitHub repository: URL: https://git.cira-lab.com/cira-medical/classification-of-avian-malaria-parasite

Acknowledgements

We are grateful to Thailand Science and Research Innovation Fund and King Mongkut's Institute of Technology Ladkrabang Fund [RE-KRIS-016-64] for providing the financial support for this research project. We are also grateful to Suchansa Thanee at the Parasitology Unit, Faculty of Veterinary Science, Chulalongkorn University, for assisting in the parasite identification. We also thank the College of Advanced Manufacturing Innovation, King Mongkut's Institute of Technology Ladkrabang which provided the deep learning platform and software to support the research project.

Author contributions

SB, VK and SC conceived and designed the research study; SB, VK, MK, KMN and SC wrote the manuscript; VK, KMN, RJ, KK and SC performed the computational experiment; MK and ST performed the parasite investigation; TT, SC and SB conducted the computer's platform. SB read and approved the final manuscript.

Competing interest

The authors declare that they have no competing interest.

References

1. Pattaradilokrat, S. *et al.* Molecular detection of the avian malaria parasite Plasmodium gallinaceum in Thailand. *Vet Parasitol* **210**, 1–9, doi:10.1016/j.vetpar.2015.03.023 (2015).
2. Bolei Zhou, A., Khosla, A., Lapedriza, A. O. & Torralba, A. Learning Deep Features for Discriminative Localization. arXiv:1512.04150v1, 1–10(2015).
3. Matek, C., Spiekermann, S. S. K. & Marr, C. Human-level recognition of blast cells in acute myeloid leukaemia with convolutional neural networks. *Nature Machine Intelligence volume.* **1**, 538–544 (2019).
4. Jiram, A. I. *et al.* Evidence of asymptomatic submicroscopic malaria in low transmission areas in Belaga district, Kapit division, Sarawak, Malaysia. *Malar J.* **18**, 156 https://doi.org/10.1186/s12936-019-2786-y (2019).
5. Raman, J. *et al.* High levels of imported asymptomatic malaria but limited local transmission in KwaZulu-Natal, a South African malaria-endemic province nearing malaria elimination. *Malar J.* **19**, 152 https://doi.org/10.1186/s12936-020-03227-3 (2020).
6. He, K., Zhang, X., Ren, S. & Sun, J. Deep Residual Learning for Image Recognition 2016 *IEEE Conference on Computer Vision and Pattern Recognition (CVPR)*, 770–778 (2016).

7. Huang, G., Liu, Z. & Weinberger, K. Q. Densely Connected Convolutional Networks 2017 *IEEE Conference on Computer Vision and Pattern Recognition (CVPR)*, 2261–2269 (2017).
8. Joseph Redmon, A. F. YOLOv3: An Incremental Improvement. arXiv:1804.02767 [cs.CV](2018).
9. Torres, K. *et al.* Automated microscopy for routine malaria diagnosis: a field comparison on Giemsa-stained blood films in Peru. *Malar J.* **17**, 339 https://doi.org/10.1186/s12936-018-2493-0 (2018).
10. Rajaraman, S., Jaeger, S. & Antani, S. K. Performance evaluation of deep neural ensembles toward malaria parasite detection in thin-blood smear images. *PeerJ.* **7**, e6977 https://doi.org/10.7717/peerj.6977 (2019).
11. Sheeba, F., Mammen, T. R. & Nagar, J. J. A.K. in *Proceedings of Seventh International Conference on Bio-Inspired Computing: Theories and Applications (BIC-TA 2012).* (ed Singh P. In: Bansal J., Deep K., Pant M., Nagar A) 289–298 (Springer).
12. Fuhad, K. M. F. *et al.* Deep Learning Based Automatic Malaria Parasite Detection from Blood Smear and its Smartphone Based Application. *Diagnostics (Basel).* **10**, https://doi.org/10.3390/diagnostics10050329 (2020).
13. 13. Unver, H. M. & Ayan, E. Skin Lesion Segmentation in Dermoscopic Images with Combination of YOLO and GrabCut Algorithm. *Diagnostics (Basel)* **9**, doi:10.3390/diagnostics9030072 (2019).
14. Wang, Q. *et al.* Deep learning approach to peripheral leukocyte recognition. *PLoS One* **14**, e0218808, doi:10.1371/journal.pone.0218808 (2019).
15. Zhuang, Z. *et al.* Cardiac VFM visualization and analysis based on YOLO deep learning model and modified 2D continuity equation. *Comput Med Imaging Graph* **82**, 101732, doi:10.1016/j.compmedimag.2020.101732 (2020).
16. Kalipsiz Oya, GÖKÇE Erhan & Pınar, C. Veterinerlik Alanında Makine Öğrenmesi Uygulamaları Üzerine Bir Derleme. *Kafkas Universitesi Veteriner Fakultesi Dergisi* **23**, 673–680, doi:10.9775/kvfd.2016.17281 (2017).
17. Bertram, C. A. *et al.* Validation of Digital Microscopy Compared With Light Microscopy for the Diagnosis of Canine Cutaneous Tumors. *Vet Pathol* **55**, 490–500, doi:10.1177/0300985818755254 (2018).
18. Awaysheh, A. *et al.* Review of Medical Decision Support and Machine-Learning Methods. *Vet Pathol* **56**, 512–525, doi:10.1177/0300985819829524 (2019).
19. Ahmed Waleed *et al.* in *2019 14th International Conference on Computer Engineering and Systems (ICCES)* 201–206 (IEEE, 2019).
20. Marzahl, C. *et al.* Deep Learning-Based Quantification of Pulmonary Hemosiderophages in Cytology Slides. *Sci Rep* **10**, 9795, doi:10.1038/s41598-020-65958-2 (2020).
21. Aubreville, M. *et al.* Deep learning algorithms out-perform veterinary pathologists in detecting the mitotically most active tumor region. *Sci Rep* **10**, 16447, doi:10.1038/s41598-020-73246-2 (2020).
22. Vinicki, K., Ferrari, P., Belic, M. & Turk, R. Using Convolutional Neural Networks for Determining Reticulocyte Percentage in Cats. arXiv:1803.04873 (2018).

<https://ui.adsabs.harvard.edu/abs/2018arXiv180304873V>.

23. Kaewkamnerd, S. *et al.* An automatic device for detection and classification of malaria parasite species in thick blood film. *BMC Bioinformatics* **13 Suppl 17**, S18-S18, doi:10.1186/1471-2105-13-S17-S18 (2012).
24. Sheeba, F., Thamburaj, R., Mammen, J. J. & Nagar, A. K. 289–298 (Springer India).
25. Pamungkas, A., Adi, K. & Gernowo, R. Identification of plasmodium falciparum development phase in malaria infected red blood cells using adaptive color segmentation and decision tree based classification. *International Journal of Applied Engineering Research* **10**, 4043–4056 (2015).
26. Preedanan, W., Phothisonothai, M., Senavongse, W. & Tantisatirapong, S. in *2016 8th International Conference on Knowledge and Smart Technology (KST).* 215–218.
27. Gopakumar, G., Swetha, M., Siva, G. S. & Subrahmanyam, G. R. K. S. in *Proceedings of the Tenth Indian Conference on Computer Vision, Graphics and Image Processing* Article 16 (Association for Computing Machinery, Guwahati, Assam, India, 2016).
28. Liang, Z. *et al.* in *2016 IEEE International Conference on Bioinformatics and Biomedicine (BIBM).* 493–496.
29. Haryanto, S. E. V., Mashor, M. Y., Nasir, A. S. A. & Jaafar, H. in *2017 5th International Conference on Cyber and IT Service Management (CITSM).* 1–4.
30. Bibin, D., Nair, M. S. & Punitha, P. Malaria Parasite Detection From Peripheral Blood Smear Images Using Deep Belief Networks. *IEEE Access* **5**, 9099–9108 (2017).
31. Hung, J. *et al.* Applying Faster R-CNN for Object Detection on Malaria Images. *ArXiv* **abs/1804.09548** (2018).
32. Bhuvan, C., Bansal, S., Gupta, R. & Bhan, A. in *2020 7th International Conference on Signal Processing and Integrated Networks (SPIN).* 1132–1135.
33. Kalkan, S. C. & Sahingoz, O. K. in *2019 Scientific Meeting on Electrical-Electronics & Biomedical Engineering and Computer Science (EBBT).* 1–4.
34. Shah, D., Kawale, K., Shah, M., Randive, S. & Mapari, R. in *2020 4th International Conference on Intelligent Computing and Control Systems (ICICCS).* 984–988.
35. Fuhad, K. M. F. *et al.* Deep Learning Based Automatic Malaria Parasite Detection from Blood Smear and its Smartphone Based Application. *Diagnostics (Basel)* **10**, 329, doi:10.3390/diagnostics10050329 (2020).
36. Dong, Y. *et al.* in *2017 IEEE EMBS International Conference on Biomedical & Health Informatics (BHI).* 101–104.
37. Valkiūnas, G. & Iezhova, T. A. Keys to the avian malaria parasites. *Malaria Journal* **17**, 212, doi:10.1186/s12936-018-2359-5 (2018).
38. Vijayalakshmi, A. & Rajesh Kanna, B. Deep learning approach to detect malaria from microscopic images. *Multimedia Tools and Applications* **79**, 15297–15317, doi:10.1007/s11042-019-7162-y (2020).

39. Yurayart, N., Kaewthamasorn, M. & Tiawsirisup, S. Vector competence of Aedes albopictus (Skuse) and Aedes aegypti (Linnaeus) for Plasmodium gallinaceum infection and transmission. *Vet Parasitol* **241**, 20–25, doi:10.1016/j.vetpar.2017.05.002 (2017).
40. Loey, M., Manogaran, G., Taha, M. H. N. & Khalifa, N. E. M. Fighting against COVID-19: A novel deep learning model based on YOLO-v2 with ResNet-50 for medical face mask detection. *Sustain Cities Soc* **65**, 102600, doi:10.1016/j.scs.2020.102600 (2021).
41. Kittichai, V. *et al.* Deep learning approaches for challenging species and gender identification of mosquito vectors. *Sci Rep* **11**, 4838, doi:10.1038/s41598-021-84219-4 (2021).
42. Li Liu, W. O., Xiaogang Wang, Paul Fieguth, Jie Chen, Xinwang Liu, Matti Pietikäinen. Deep Learning for Generic Object Detection: A Survey. *International Journal of Computer Vision* **128**, 261–318, doi:https://doi.org/10.1007/s11263-019-01247-4 (2020).
43. Nhat-Duy Nguyen, T. D., Thanh Duc Ngo, and Duy-Dinh Le. An Evaluation of Deep Learning Methods for Small Object Detection. *Journal of Electrical and Computer Engineering* **2020**, 1–18, doi:https://doi.org/10.1155/2020/3189691 (2020).
44. Joseph Redmon & Farhadi, A. *Darknet: Open Source Neural Networks in C*, <http://pjreddie.com/darknet/> (2013–2016).
45. Bolei Zhou, Aditya Khosla, Agata Lapedriza, Aude Oliva & Torralba, A. Learning Deep Features for Discriminative Localization. *arXiv:1512.04150v1*, 1–10 (2015).
46. Christian Matek, S. S., Karsten Spiekermann, and Carsten Marr. Human-level recognition of blast cells in acute myeloid leukaemia with convolutional neural networks. *Nature Machine Intelligence volume* **1**, 538–544 (2019).
47. Jiram, A. I. *et al.* Evidence of asymptomatic submicroscopic malaria in low transmission areas in Belaga district, Kapit division, Sarawak, Malaysia. *Malar J* **18**, 156, doi:10.1186/s12936-019-2786-y (2019).
48. Raman, J. *et al.* High levels of imported asymptomatic malaria but limited local transmission in KwaZulu-Natal, a South African malaria-endemic province nearing malaria elimination. *Malar J* **19**, 152, doi:10.1186/s12936-020-03227-3 (2020).
49. He, K., Zhang, X., Ren, S. & Sun, J. Deep Residual Learning for Image Recognition. *2016 IEEE Conference on Computer Vision and Pattern Recognition (CVPR)*, 770–778 (2016).
50. Huang, G., Liu, Z. & Weinberger, K. Q. Densely Connected Convolutional Networks. *2017 IEEE Conference on Computer Vision and Pattern Recognition (CVPR)*, 2261–2269 (2017).
51. Joseph Redmon, A. F. YOLOv3: An Incremental Improvement. *arXiv:1804.02767 [cs.CV]* (2018).
52. Torres, K. *et al.* Automated microscopy for routine malaria diagnosis: a field comparison on Giemsa-stained blood films in Peru. *Malar J* **17**, 339, doi:10.1186/s12936-018-2493-0 (2018).
53. Rajaraman, S., Jaeger, S. & Antani, S. K. Performance evaluation of deep neural ensembles toward malaria parasite detection in thin-blood smear images. *PeerJ* **7**, e6977, doi:10.7717/peerj.6977 (2019).

54. Sheeba F., T. R., Mammen J.J., Nagar A.K. in *Proceedings of Seventh International Conference on Bio-Inspired Computing: Theories and Applications (BIC-TA 2012)*. (ed Singh P. In: Bansal J., Deep K., Pant M., Nagar A) 289–298 (Springer).

55. Fuhad, K. M. F. *et al.* Deep Learning Based Automatic Malaria Parasite Detection from Blood Smear and its Smartphone Based Application. *Diagnostics (Basel)* **10**, doi:10.3390/diagnostics10050329 (2020).

Figures

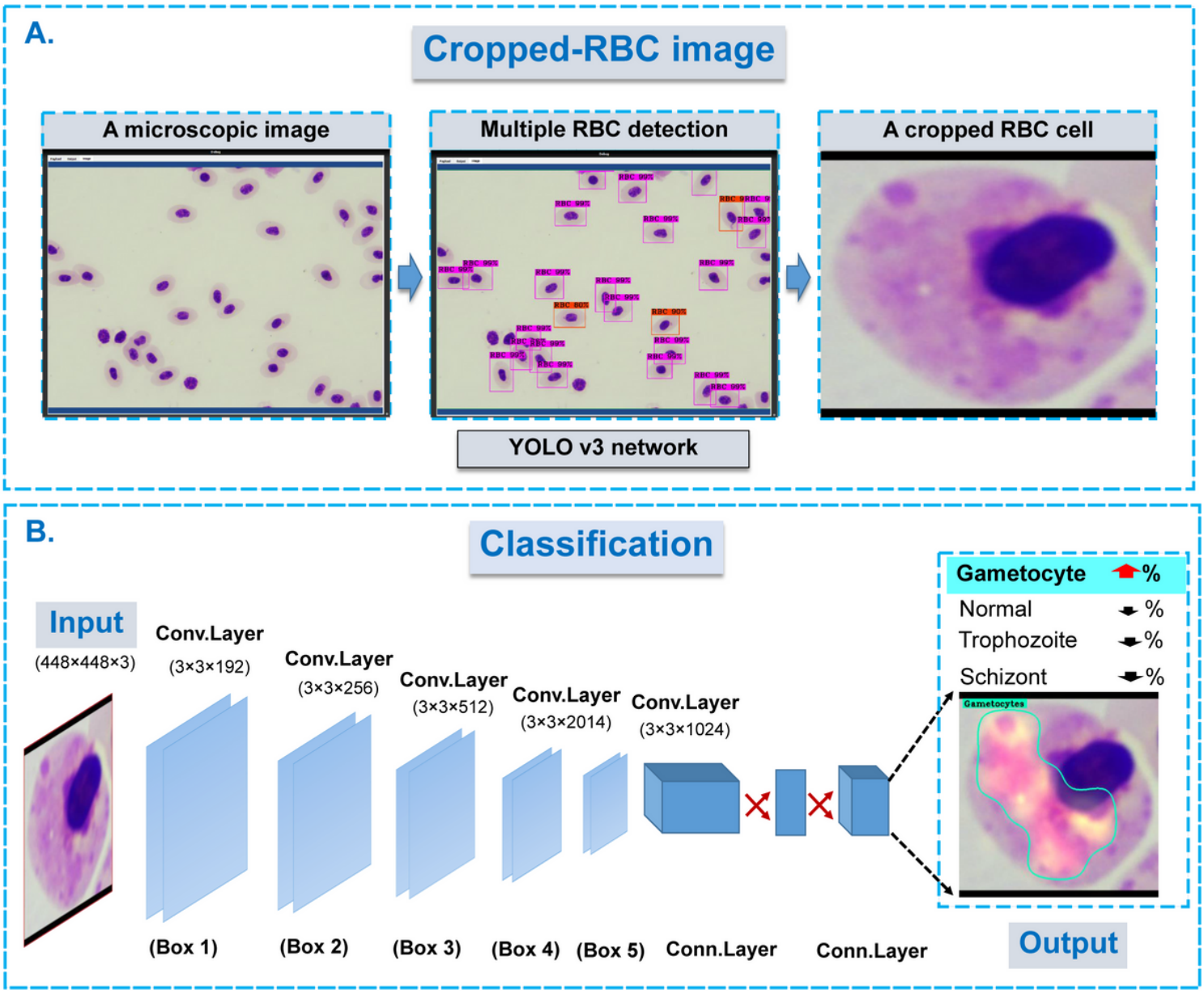

Figure 1

The schematic of the two-state learning strategies for classification of the single chicken's RBC-cell infected by P. gallenaceum. (A) A microscopic image with multiple RBC infected malaria stages was

captured under oil immersion field (1000× magnification). An individual RBC cells were cropped under CiRA CORE platform if these cells were correctly detected by well-trained YOLO v3 model. (B) Each cropped-RBC cell with/ without malaria infection was then classified by trained image classification networks including Darknet, Darknet19, Darknet19-448 and Densenet201, respectively. Filters each convolution layer help generate an attention map in the part of feature extraction. The attention map of the JET color gradient is used to visualize self-region of the interest of the input based on optimal weight.

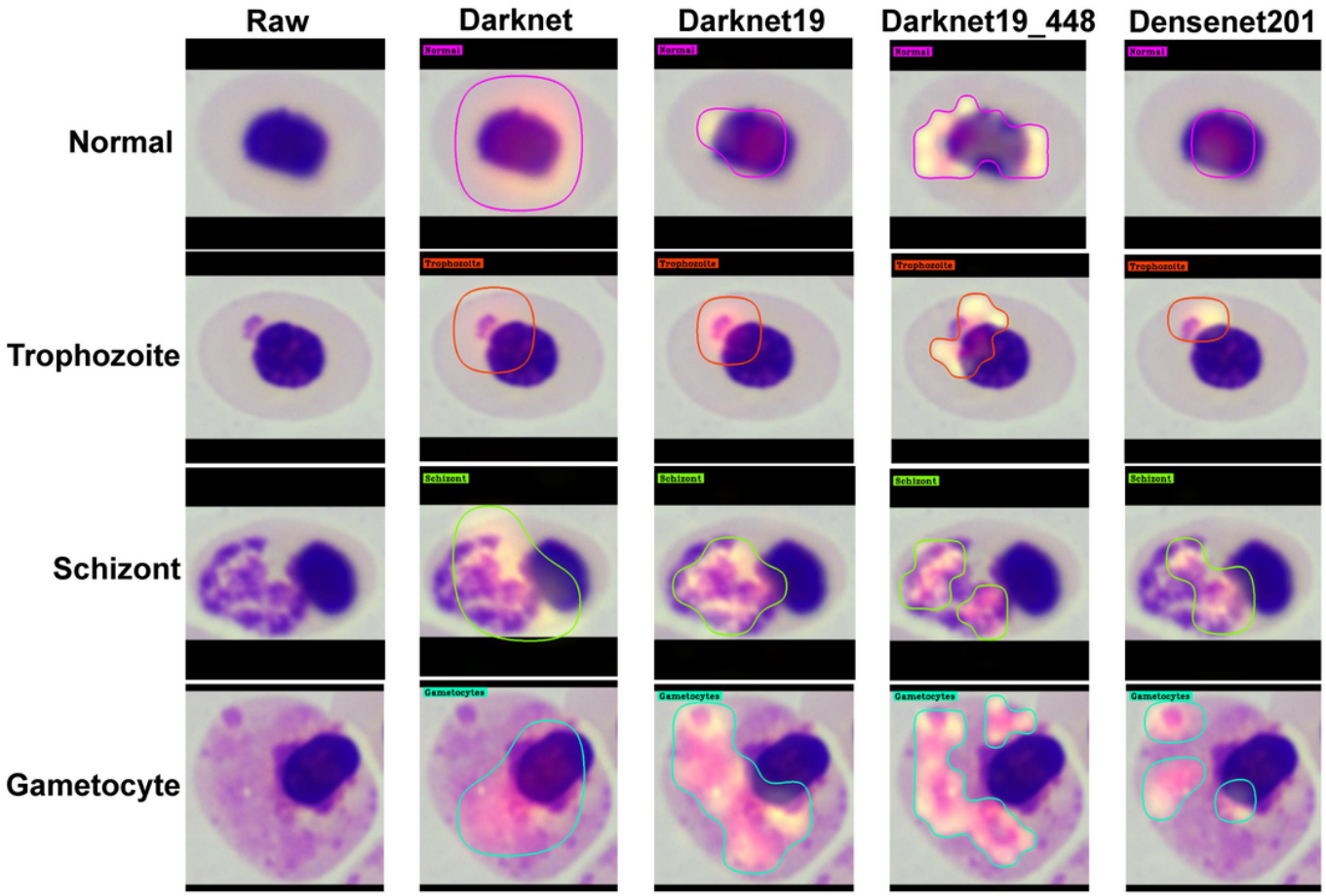

Figure 2

Prediction labeling of the outcome through all four selectable models. The color of the attention map indicated the field of interest predicted by each model. The X-axis is the input image and following the study models such as Darknet, Darknet19, Darknet19-448 and Densenet201. Y-axes are individual chicken-blood cells that are regular and those that are infected malaria, including trophozoites, schizonts and gametocytes.

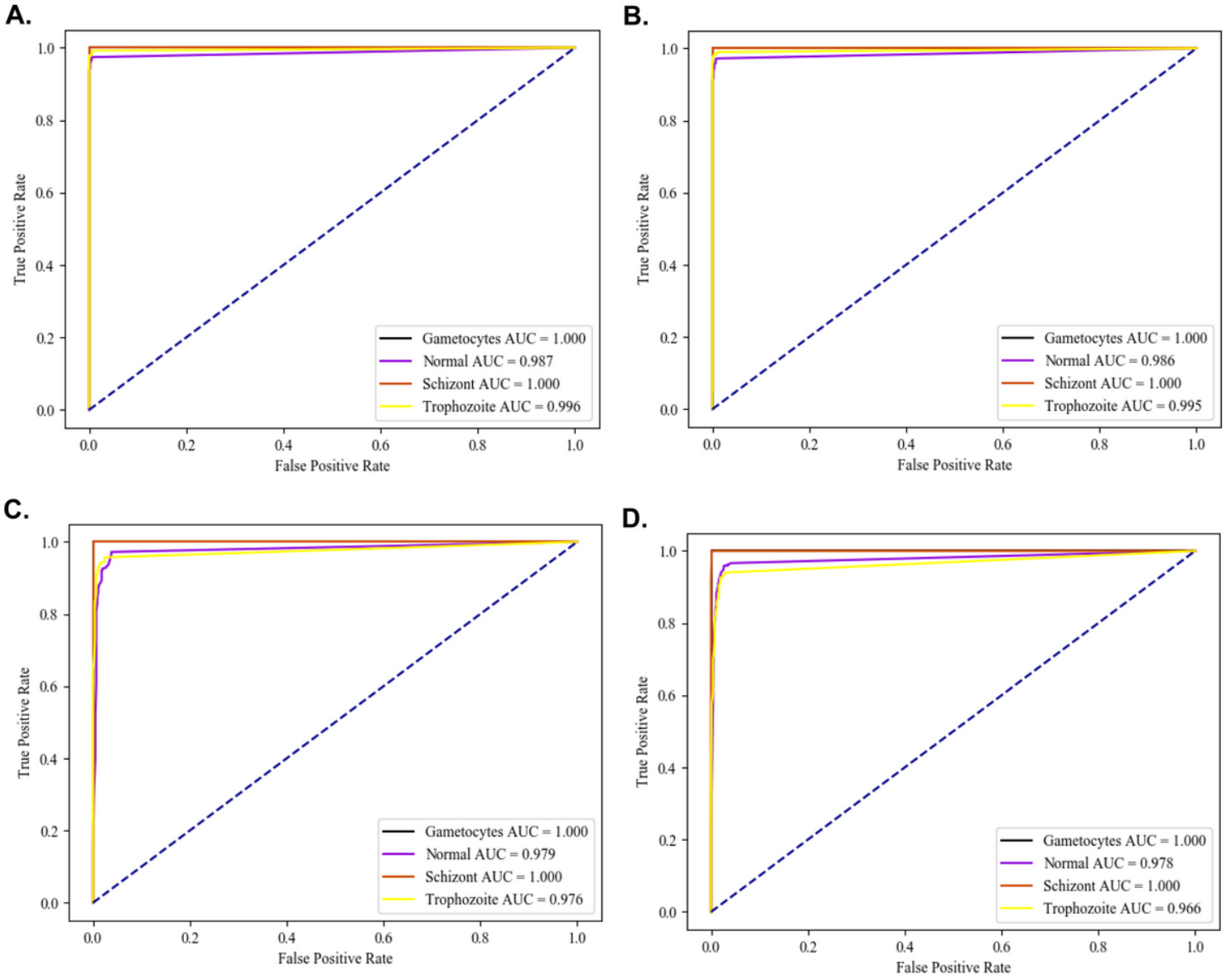

Figure 3

The AUC under the ROC curve analyzed by the model- wise performance following; A. Darknet, B. Darknet19, C.Darknet19_448 and D. Densenet201, respectively. Besides, the plot also present class-wise comparison following; Gametocyte, Normal RBC, Schizont and Trophozoite, respectively.

Supplementary Files

This is a list of supplementary files associated with this preprint. Click to download.

- Supplementary.docx
- avianmalariaparasitePlasmodiumgallinaceumbloodstages.mp4